DOI: 10.1002/fuce.201900201

PBI-type Polymers and Acidic Proton Conducting Ionic Liquids – Conductivity and Molecular Interactions▲

J. Lin[1,2], C. Korte[1,2]*

[1] Forschungszentrum Jülich GmbH, Institute of Energy and Climate Research – Electrochemical Process Engineering (IEK-14), Wilhelm-Johnen-Straße, 52425 Jülich, Germany
[2] RWTH Aachen University, 52062 Aachen, Germany

Received November 25, 2019; accepted June 25, 2020; published online August 10, 2020

Abstract

Proton conducting ionic liquids (PILs) are discussed as new electrolytes for the use as non-aqueous electrolytes at operation temperatures above 100 °C. During fuel cell operation the presence of significant amounts of residual water is unavoidable. The highly Brønsted-acidic PIL 2-Sulfoethylmethylammonum triflate [2-Sema][TfO] is able to perform fast proton exchange processes with H_2O, resulting from ^{1}H-NMR and pulsed field gradient (PFG)/diffusion ordered spectroscopy (DOSY) self-diffusion measurements. Proton conduction takes place by a vehicle mechanism *via* PIL cations or H_3O^+, but also by a cooperative mechanism involving both species. Thus, highly Brønsted-acidic PILs are promising candidates for the use as non-aqueous electrolytes. To use [2-Sema][TfO] as electrolyte in a proton electrolyte fuel cell (PEFC) it has to be immobilized in a host polymer. There is a (slow) uptake of the PIL by polybenzimidazole (PBI) up to a weight increase of ~130%, due to a swelling process. A protonation of the basic imidazole moieties takes place. NMR analysis was applied to elucidate the molecular interactions between PBI, PIL, and residual water. Proton exchange, respectively an interaction between the polar groups and water can be observed in spectra, indicating a network of H-bonds in doped PBI. Therefore, highly acidic PILs are promising candidates for the use as non-aqueous electrolytes.

Keywords: HT-PEFC, Ionic Liquids, PEFCs for Operation >100 °C, Polymers, Proton Exchange Membranes, Proton Transport

1 Introduction

Polymer electrolyte fuel cells (PEFCs), operational at an elevated temperature above 100 °C, have attracted much attention recently, due to their superiorities compare to low temperature (LT)-PEFCs: (i) no feed gas humidification, (ii) a more efficient cooling system (easier water and heat management), (iii) the possibility of recovering high-grade waste heat, and (iv) a higher tolerance against feed gas impurities [1, 2]. Currently, (high temperature) HT-PEFC, based on phosphoric acid doped polybenzimidazole (PBI) membranes, cannot compete with the performance characteristics of NAFION-based LT-PEFCs [3]. Despite the high operation temperature of 160 °C, the presence of H_3PO_4 causes a slow cathodic oxygen reduction reaction kinetics (ORR). This is primarily caused by an inhibition effect due to a poisoning by adsorption of H_3PO_4 species onto active catalyst sites [4]. Also discussed is a low solubility of O_2 and a slow diffusion of O_2 through the H_3PO_4 film which covers the platinum catalyst [5]. Thus, there is a necessity for new non-aqueous proton conducting electrolytes operational for the temperature range between 100–120 °C.

PBI is widely used in HT-PEFCs as a proton-conducting electrolyte matrix, because of its high decomposition temperature and excellent thermal and chemical stability. The basic imidazole moieties of the PBI chains are protonated by H_3PO_4, the

▲ *Paper presented at the 23rd EFCF Conference ''Low-Temperature Fuel Cells, Electrolyzers, H2-Processing Forum'' (EFCF2019), 2–5 July 2019 held in Lucerne, Switzerland. Organized by the European Fuel Cell Forum www.efcf.com*

[*] *Corresponding author, c.korte@fz-juelich.de*

$H_2PO_4^-$ anions interact with the polymer chains by strong coulomb forces and the additional H_3PO_4 molecules by H-bonds [6]. Mobile charge carriers for protons are formed by a strong autoprotolysis, i.e., $H_4PO_4^+$ and $H_2PO_4^-$, hence providing a high proton conductivity at low water concentrations.

Proton conducting ionic liquids (PILs) with acidic cations are promising candidates for the use as non-aqueous electrolytes at operation temperatures above 100 °C and got much attention for applications in PEFCs [7]. PILs are ionic compounds with bulky cations and anions [8]. PILs with anions based on very strong acid respectively super acids as trifluoromethanesulfonic acid or bis-trifluoromethylsulfonimid have a less inhibiting effect than H_3PO_4 because these anions, e.g., triflate $CF_3SO_3^-$ or triflimid $(CF_3SO_2)_2N^-$, are less strongly adsorbed on Pt than H_3PO_4 or $H_2PO_4^-$.

In a neat (i.e., water-free) PIL, proton transport can inevitably only take place by a vehicle mechanism. However, PILs are normally hygroscopic. During fuel cell operation, also above 100 °C, a water uptake will unavoidably take place. On the other hand, by utilising the hygroscopicity of the PIL and the water production at the cathode side of the fuel cell, a way to enhance the conductivity of the electrolyte may be provided. The amphoteric water will act as a proton acceptor and donor and participates in the proton transfer processes in the bulk of the PIL as a fast carrier.

In this contribution we present an experimental study on the proton transport mechanism in a high Brønsted-acidic PIL as a function of the amount of residual water. Moreover, the interaction of the high acidic PIL with a host polymer with basic moieties like *m*-PBI is investigated to ascertain its ability as a possible membrane material. A PIL with a high acidic cation, 2-Sulfoethylmethylammonum triflate [2-Sema][TfO] is prepared. The ability to protonate the residual H_2O were investigated by mixing appropriate amounts of the PIL and H_2O at various molar ratios to obtain compositions varying from neat PIL to H_2O-excess conditions. The interactions between PIL cation and H_2O were determined by measuring the macroscopic (total) conductivity and the self-diffusion coefficients by ^{1}H-NMR spectroscopy (PFG/DOSY). The neat PIL is introduced into PBI polymer membrane by a doping (swelling) process. The PIL uptake degree was monitored by the weight increase. The doping process was monitored by infrared (IR) spectroscopy, proving the protonation of base imidazole groups on PBI chains. Thermogravimetric alanysis (TGA) measurements were used to determine the thermal stability of the doped membranes.

2 Experimental

2.1 Ionic Liquid Preparation

[2-Sema][TfO] was prepared by slowly adding trifluoromethanesulfonic acid (reagent grade, 98%, Sigma Aldrich) to 2-methylaminoethansulfonic acid (N-methyltaurine, ≥99%, Sigma Life Science). A more detailed description of the preparation process can be found elsewhere [9]. Coulometric Karl-Fischer titration (852 Titrando/Metrohm company) yielded a water concentration of 0.6 wt.%. By adding appropriate amounts of water, various compositions from neat to equimolar ratio between PIL and H_2O molecules were achieved. In the case of [2-Sema][TfO], a water concentration of ~6 wt.% corresponds to an equimolar ratio, i.e., 50 mol.% H_2O.

2.2 ^{1}H-NMR Parameters

The acquisition of the NMR spectra was performed by using a Bruker 600 MHz spectrometer, equipped with a 5 mm cryoprobe tuned to ^{1}H. The chemical shifts were determined by using an external deuterium reference (field lock), i.e., capillaries filled with D_2O and enclosed together with the PIL in the sample tubes. The measurements were conducted at 90 °C to achieve a lower viscosity compared to room temperature.

The NMR samples of the membranes were dissolved in DMSO-d6 and filled in 5 mm tube. The measurements were conducted at room temperature (25 °C).

2.3 Measurement of the Diffusion Coefficients

The self-diffusion coefficients were measured by using the PFG/DOSY technique. The applied parameters were: 3.5 ms diffusion gradient length (δ), 100 ms diffusion delay (Δ), 15 gradient increments with gradient strength (g) from 1.3 to 32.5 G cm^{-1}. The combination of δ and Δ was optimized to give rise to at least 85% signal attenuation at strongest gradient field.

2.4 Ionic Liquid Doped Membrane Preparation

PBI membranes with a thickness of 60 µm (un-doped) were cut into samples of ~5 cm^2. The membrane samples were predried by a heat treatment at 150 °C for 30 min. The membranes were immersed in the neat PILs for a doping (swelling) process at various temperatures to investigate the uptake kinetics. The membrane samples were weighed before and after immersion to obtain the mass difference. The uptake degree was calculated by the weight increase, as given in Eq. (1):

$$uptake\ degree = \frac{m_b - m_a}{m_a} \cdot 100\% \quad (1)$$

where m_a and m_b are the mass of original dried PBI membrane and the after doping membrane, respectively.

2.5 Membrane Characterization

Attenuated total reflection (ATR) spectra of the undoped and doped membrane samples and of the neat PIL were measured in reflection mode in the range of 500–4,000 cm^{-1} (Monolithic diamond GladiATR, PIKE technologies). The experiments were carried out at room temperature. The thermal stability of the membranes and PIL were examined, by using TGA (Perkin Elmer STA 6000). The samples were heated from room temperature to 800 °C with a heating rate of 5 °C min^{-1} in air atmosphere. Weight loss was measured and reported as a

function of temperature. The baseline correction was performed by using an empty crucible and an identical measurement program. The images of membranes were taken by a light microscope (ZEISS AXIO Imager, M1m).

3 Results and Discussion

3.1 (Total) Conductivity vs. Temperature and H_2O Concentration

To investigate the influence of the water content on the proton transport in the PIL, 2–6 wt.% H_2O was added. This corresponds to a molar ratio of 25–50 mol.% H_2O. The conductivity data were reported in our previous work [10]. The AC conductivity measurements were performed in a four-probe conductivity cell, using platinum electrodes. The total ohmic resistance was determined by means of impedance spectroscopy. The dependency of the (total) conductivity σ in the [2-Sema][TfO]/H_2O system on the temperature T of nearly neat [2-Sema][TfO] up to a ratio of 50 mol.% H_2O is shown in Figure 1. The conductivity depends on the H_2O content w_{H_2O} and the temperature T. In the range of 60–100 °C no distinct Vogler-Tammann-Fulcher (VTF) behavior is observed. The activation energy E_a decreases considerably from 44.9 kJ mol^{-1} for the neat PIL to 37.6 kJ mol^{-1} for a molar ratio of 50 mol.% H_2O.

Both, an increasing temperature T and an increasing H_2O concentration lead to a decrease of the viscosity of a PIL. In the case of pure vehicular charge transport, the conductivity is coupled *via* the Stokes-Einstein relation to the (dynamic) viscosity η. However, due to the high acidity of the [2-Sema]$^+$ cation, a significant amount of the cations undergo an intermolecular proton transfer to the residual water molecules , as given in Eq. (2):

$$CH_3NH_2{}^+CH_2CH_2SO_3H + H_2O = CH_3NH_2{}^+CH_2CH_2SO_3{}^- + H_3O^+ \quad (2)$$

Considering the pK_A values of H_3O^+ and of a SO_3H moiety, the equilibrium concentration of H_3O^+ is most likely in the same order of magnitude as the concentration of the remaining [2-Sema]$^+$ cations. Due to the protolysis equilibrium, the proton transport in the PIL/H_2O systems can take place not only by the migration of the cation but also of the H_3O^+ ions. It can assumed that the mobility of the smaller H_3O^+ ions is higher than that of the cation. Thus, more mobile charge carriers are formed with increasing H_2O concentration. Alternatively, an cooperative proton transport mechanism can take place, due to a fast excange of protons between H_3O^+, H_2O, [2-Sema]$^+$ and N-Methyltaurine. The change of the activation energy *vs.* H_2O concentration indicates either a change of the predominating charge carrier or of the mechanism. To decide this, ^{1}H-NMR measurements were performed.

3.2 ^{1}H-NMR and Self-diffusion Coefficients

The prevailing mobile charge carrier, respectively the proton transport mechanism, can be evidenced by performing ^{1}H-NMR measurements and using the PFG/DOSY technique to gain information about the self-diffusion coefficients of each protonic species. The chemical shifts δ of individual protons of the [2-Sema]$^+$ cation in the [2-Sema][TfO]/H_2O system, gained from the ^{1}H-NMR spectra, are shown in Figure 2 as a function of the H_2O content w_{H_2O}. The ^{1}H-NMR spectrum of (nearly) neat [2-Sema][TfO] at room temperature is shown exemplarily in Figure 7.

The two signals of (nearly) neat [2-Sema][TfO], appearing at high magnetic fields at a shift of 3.4 and 4.1 ppm, can be assigned to the CH_3 and CH_2CH_2 protons and the signal at a medium field of 7.5 ppm is assigned to the NH_2 protons. The acidic proton of the SO_3H group appears at a low magnetic field and a shift of 12.9 ppm. With increasing H_2O content w_{H_2O}, up to an equimolar composition (~6 wt.%), it shifts about 1.9 ppm towards a higher field.

The latter observation can be caused by strong interactions between the high acidic protons of the [2-Sema]$^+$ cations and the H_2O molecules. If the kinetic of the proton exchange between the SO_3H group and the H_3O^+ ions is very fast, both species cannot be separated by ^{1}H-NMR. This results in a single signal at an averaged position. Adding H_2O will increase the H_3O^+ concentration in the protolysis equilibrium because of the high acidity of the [2-Sema]$^+$ cations and will increase the total concentration of the active (mobile) protons.

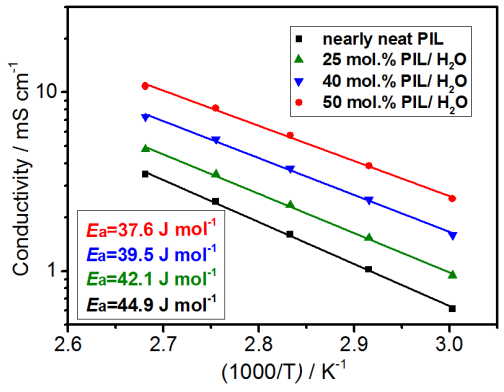

Fig. 1 (Total) conductivity of nearly neat to 50 mol.% H_2O concentration [2-Sema][TfO] *vs.* temperature T.

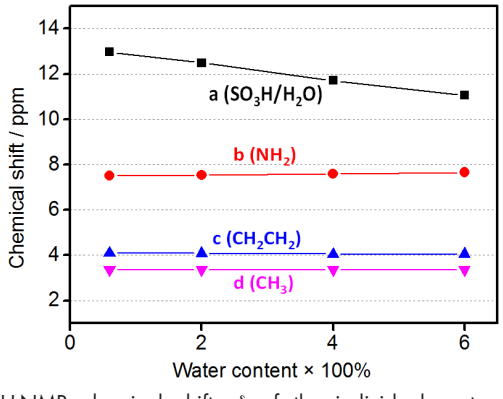

Fig. 2 ^{1}H-NMR chemical shifts δ of the individual protons of the [2-Sema]$^+$ cation in the [2-Sema][TfO]/H_2O system *vs.* the H_2O content w_{H_2O}.

As the protons of H_3O^+ ions can be expected at a lower field than the protons of H_2O molecules and at a higher field than the protons of SO_3H groups [11], this may lead to the observed shift to a higher field and in an increase of the relative integral peak intensity (area).

The proton self-diffusion coefficients D_i of the different protonic species were measured by using the PFG/DOSY technique. In Figure 3 the evaluated self-diffusion coefficients for a temperature of 90 °C are shown as a function of the H_2O content. Because of the high viscosity of [2-Sema][TfO], the DOSY measurements were at this elevated temperature for a more precise measurement of the relaxation time.

The self-diffusion coefficient D_{SO_3H/H_2O} the of active (acidic) proton differs from the self-diffusion coefficient $D_{NH_2^+}$, $D_{CH_2CH_2}$, and D_{CH_3} of the other protons attached to the cation, see Figure 3. In the whole investigated H_2O concentration range the active proton diffuses distinctly faster than other protons. With increasing H_2O content, the self-diffusion coefficient of all protons are increasing, but in the case of the active proton (SO_3H/H_2O) the increase (slope) is much higher compared to the others (NH_2^+, CH_2CH_2 and CH_3).

When extrapolating to ideally neat [2-Sema][TfO], i.e., $w_{H_2O} = 0$, the difference between the self-diffusion coefficients vanishes. This confirms to the assumption made above on the possible transport mechanisms in a high acidic PIL. In the neat PIL the proton transport is restricted to the diffusional motion of the whole cation. A pure vehicle mechanism is present. A value of $(7 \pm 2) \cdot 10^{-8}\,cm^2\,s^{-1}$ can be estimated for the $[2\text{-Sema}]^+$ cation in neat [2-Sema][TfO].

With increasing H_2O concentration and increasing concentration of H_3O^+ due to protolysis, more mobile charge carriers are present. Moreover, due to a fast exchange of the proton between $[2\text{-Sema}]^+$ and H_3O^+, the predominating proton transport mechanism changes from vehicular to cooperative. The increase of the self-diffusion coefficients of the other protons may be only caused by the change of the viscosity, as already discussed above.

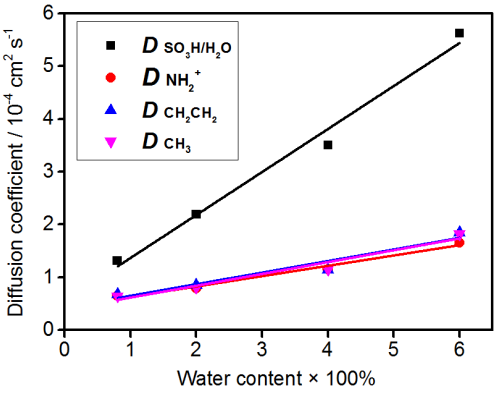

Fig. 3 Self-diffusion coefficients of the different protonic species of [2-Sema][TfO] *vs.* the H_2O content at a temperature of 90 °C.

3.3 Uptake of PILs by m-PBI by a Swelling Process

There is a slow uptake of neat [2-Sema][TfO] by *m*-PBI, when performing a swelling experiment with a membrane sample. The doping process is strongly dependent on the doping temperature. The degree of uptake (increase in wt.%) at various doping temperatures T depends on the doping time t according to Fick's 2nd law, as depicted in Figure 4. Thus, a higher temperature provides a faster doping process. However, the uptake reaches a certain limitation of about 125 to 135 wt.%. From the temperature dependence of the diffusion process, an activation energy E_a of 122.7 kJ mol^{-1} can be estimated. Using a four-probe setup the obtained membranes exhibit a (total) conductivity of 2.68 mS cm^{-1} at 100 °C and 30% rel. humidity (RH).

The diffusion coefficients $\tilde{D}_{[2\text{-Sema}][TfO]}$ evaluated from the doping process are depicted in Table 1. The Fick's diffusion coefficient $\tilde{D}_{[2\text{-Sema}][TfO]}$ of [2-Sema][TfO] in *m*-PBI at a temperature of 100 °C has a value of about $1.9 \cdot 10^{-10}\,cm^2\,s^{-1}$. This is 3 orders of magnitude lower compared to the analogue doping process with H_3PO_4 [12]. This may be caused by the apparent bigger molecular size of [2-Sema][TfO] and a spatial steric hindrance.

The same doping experiment of *m*-PBI is performed with the medium acidic PIL 1-Ethylimidazole triflate [1-EIm][TfO] ($pK_a = 7.26$), and the low acidic PIL, Diethylmethylammonium triflate [Dema][TfO] ($pK_a = 10.55$)[10]. No uptake of these PILs can be detected. The uptake of a PIL by a PBI-type polymer may be highly dependent on the cation acidity, and thus on the ability to protonate the basic imidazole moieties.

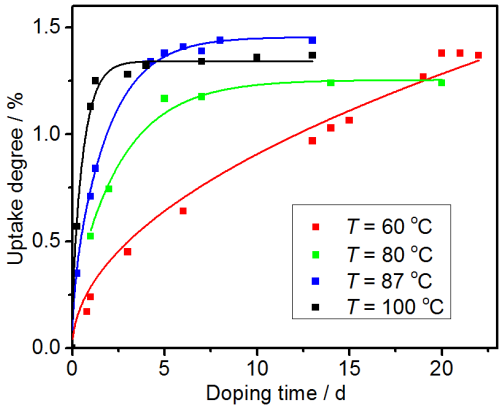

Fig. 4 Uptake degree of [2-Sema][TfO] by *m*-PBI per repeating unit as a function of doping time *t* at various temperatures *T*.

Table 1 The diffusion coefficient of [2-Sema][TfO] in *m*-PBI from the doping process.

Temperature / °C	60	80	87	100
$\tilde{D}_{[2\text{-Sema}][TfO]}$ / cm^2 s^{-1}	1.7×10^{-12}	4.4×10^{-11}	6.0×10^{-11}	1.9×10^{-10}

3.4 IR Spectra of [2-Sema][TfO] and [2-Sema][TfO] Doped PBI Membranes

The doping process of [2-Sema][TfO] into *m*-PBI was monitored by IR-ATR spectroscopy. The IR-ATR spectra of the PBI membrane, [2-Sema][TfO] and the [2-Sema][TfO] doped PBI membrane are depicted in Figure 5. In the case of the pure *m*-PBI sample, the band at 3,415 cm^{-1} is attributed to the isolated N–H stretching mode of the imidazole, i.e., non-hydrogen bonded "free" N–H groups, whereas the bands at 3,250–2,500 cm^{-1} are assigned to the stretching modes of self-associated N–H bonds [13]. The N^+-H vibrations will appear in this range, because of the protonation of the imine in the doped samples [14]. The C=N stretching mode in the imidazole ring appears in the region of 1,606 cm^{-1}. A band at 1,534 cm^{-1} is attributed to the in-plane deformation of the benzimidazole rings [15].

In the case of [2-Sema][TfO], there are no studies available concerning vibrational spectroscopy. The IR bands belonging to vibration modes of the triflate anion can be readily assigned by comparing, e.g., with literature data of aqueous sodium triflate or other triflate based ILs [16, 17]. When considering the standard textbooks, the band at ~3,200 cm^{-1} in neat [2-Sema][TfO] may be assigned to the O–H stretching mode of SO_3H group in the cation and the band at ~2,850 cm^{-1} to the N^+–H or C–H stretching modes. The bands which show up at 1,280 and 1,020 cm^{-1} can be assigned to the asymmetric and symmetric stretching modes of the SO_3 moiety of the triflate anion. The asymmetric and symmetric stretching modes of the CF_3 moiety show up at 1,210 and 1,164 cm^{-1}. As well, the bands appearing at 632 and 512 cm^{-1} can be assigned to the anion, caused by the symmetric and asymmetric deformation vibration of the SO_3 moiety [18–20]. Thus, only the remaining bands at 573, 728, 910, 1,354, and 1,469 cm^{-1} are most probably caused by vibration modes of the cation.

The spectral region of the O-H and N-H stretching modes as shown in Figure 5, reveals the evolution of the protonation of the polymer by the PIL. In the doped samples, the broad band of the N^+–H stretching mode at 3,250–2,500 cm^{-1} becomes stronger. Simultaneously, it shows a shift to lower wavenumbers, which may indicates an increasing fraction of H-bonded species [21]. The band which appears at 3,400 cm^{-1} can be probably attributed to the association of O–H from both cation and residual H_2O. The C=N stretching mode at 1,606 cm^{-1} and the C–C stretching mode at 1,534 cm^{-1} of the imidazole ring are shifting towards higher wavenumbers to 1,632 cm^{-1} and 1,578 cm^{-1}, respectively. This may be caused by the protonation of imidazole ring. The increasing electron density on carbon of the heterocycle leads to a raising absorption frequencies of ring vibrations [22].

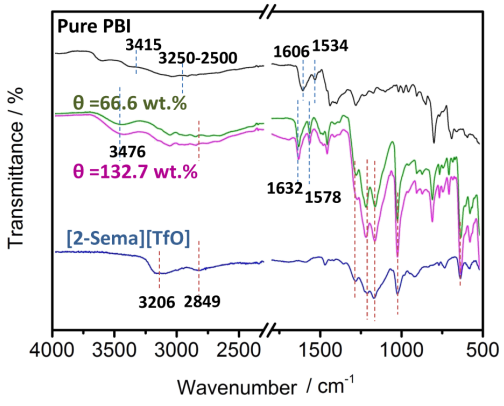

Fig. 5 The ATR spectra of PBI, [2-Sema][TfO] and doped *m*-PBI with a uptake degree of 66.6 wt.% and 132.7 wt.%.

3.5 TGA Analysis of [2-Sema][TfO] and [2-Sema][TfO] Doped PBI Membranes

The thermal properties of neat *m*-PBI and [2-Sema][TfO], as well as of TfOH and [2-Sema][TfO] doped *m*-PBI membranes are investigated by TGA, as depicted in Figure 6. TfOH doped *m*-PBI membranes were also prepared. By comparing with the [2-Sema][TfO] doped *m*-PBI membranes this allows a limited insight into the absorption stages, respectively to the composition. For doping *m*-PBI with TfOH, aqueous solutions with a concentration of 20 wt.% were used to keep control to the process and avoid a complete dissolution of the polymer material.

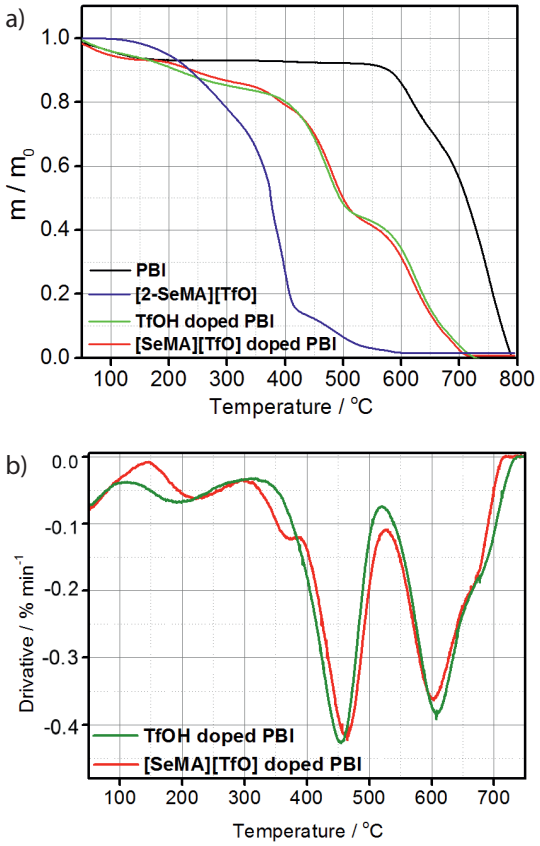

Fig. 6 The (a) TGA curves of *m*-PBI, [2-Sema][TfO], TfOH doped *m*-PBI (130 wt.%, *m*-PBI-H_2^+ $(TfO^-)_2$ · 0.61 TfOH) and [2-Sema][TfO]doped PBI (130 wt.%, *m*-PBI-H_2^+ $(TfO^-)_2$ · 0.34 [2-Sema][TfO]) and the (b) DTG curves of latter two.

Neat *m*-PBI shows an excellent thermal stability, the polymer starts to decompose beginning from 570 °C. The weight loss below 150 °C might be attributed to residual water and solvent. In the case of neat [2-Sema][TfO] a weight loss of about 5 wt.% took place between 120 °C and 197 °C. This notable low decomposition temperature might be caused by the high acidity of the cation. As discussed, the residual water is subject to a protolysis equilibrium with the cation. The hydrate of triflic acid (i.e., hydroxonium triflate) is appreciable volatile (T_b = 218–219 °C) [21–23]. Alternatively, the anion may be re-protonated by the cation, leading to a direct loss of TfOH (T_b = 162 °C) [24].

In the case of TfOH doped *m*-PBI the polymer chains were fully protonated by TfOH, as known for H_3PO_4 doped *m*-PBI, because of its high acidity [22]. Thus, a weight increase of about 98 wt.% can be predicted, assuming 2 TfO^- anions per *m*-PBI repeating unit. In the obtained "polybenzimidazolium triflate" *m*-PBI-H_2^+ $(TfO^-)_2$, the triflate anions are subject to coulombic interactions. Actually, a weight increase of about 130 wt.% is observed, i.e., there is an excess of about 30 wt.% TfOH. The excess TfOH may interact with the *m*-PBI chain by forming weak H-bonds. When considering the extent of the steps in the TGA, the weight losses in the DTG curve at 200 °C, 460 °C, and 600 °C can be attributed to the loss of excess (free) TfOH, the decomposition of the polybenzimidazolium triflate, leading to a loss of the coulombic interacting TfO^- and finally a complete decomposition of the *m*-PBI chains.

The TGA and the derivative thermogravimetric (DTG) curves of [2-Sema][TfO] doped and TfOH doped *m*-PBI membranes nearly coincide above 400 °C. Thus, the decomposition of the polybenzimidazolium triflate and the complete decomposition of the polymer are in common. In the case of [2-Sema][TfO] doped *m*-PBI the DTG curves show an extra decomposition step 380 °C.

These observations indicate that the chains of the *m*-PBI were fully protonated by the acidic cation of the ionic liquid [2-Sema][TfO]. The observed weight increase of 130 wt.% during the doping process would correspond to a doping degree of 1.44 formula units [2-Sema][TfO] per repeating unit of the polymer. The weight change in the TGA curve at 380 °C does not correlate to this. It is too small for a true PIL doping degree of 1.44. This may indicate that neutral N-methyltaurine, formed by the protolysis of the $[2\text{-Sema}]^+$ cation to the polymer chains, diffuses out. The TfO^- anions remains in the membrane, forming polybenzimidazolium triflate. According to the initial weight increase of 130 wt.% and the weight losses at 380 °C and 460 °C, the [2-Sema][TfO] doped *m*-PBI membranes actually consist of polybenzimidazolium triflate *m*–PBI–H_2^+ $(TfO^-)_2$ and about 30 wt.% [2-Sema][TfO] or residual N-methyltaurine, which might be absorbed by forming H-bonds.

The uptake of a PIL by *m*-PBI membrane in a swelling process is dependent on the acidity of cation. The protonation of *m*-PBI chain is obviously a prerequisite for the uptake of an electrolyte. In the case of the medium acidic PIL [1-EIm][TfO] and the very low acidic PIL [Dema][TfO] no interaction with *m*-PBI is observed, i.e., there is no uptake by/weight increase of the polymer ($pK_A^{cation} < pK_A^{BImH+} = 5.6$).

3.6 NMR Analysis of [2-Sema][TfO] and [2-Sema][TfO] Doped PBI Membranes

The composition of the [2-Sema][TfO] doped *m*-PBI, indicated by the TGA measurements, can be proved by ^1H and ^{13}C NMR, as shown in Figure 7. In the case of neat *m*-PBI, the seven protons of a repeating unit have all different chemical shifts. The prominent ^1H-NMR signals **a** at 13.3 ppm can be attributed to the N-H proton of the imidazole ring and the signal **b** at 9.2 ppm to the C-H proton of the benzene ring in *ortho* position to both substituents, respectively. The other aromatic C-H protons can be found in a group at around 8 ppm. The signals at 1–3 ppm can be attributed to the impurity and residual solvent. In the case of neat [2-Sema][TfO] the proton of the sulfonic acid group **f** can be found at 12.3 ppm, the protons of the amino group **e** at 6.8 ppm, the ethylene protons **c** at 3.4 ppm and the methyl protons **d** at 2.7 ppm. Because of the high viscosity of [2-Sema][TfO], the FWHM of the signals is comparable high (~0.5 ppm). Thus, no multiplets due to J-coupling are detectable.

In the case of the spectra of [2-Sema][TfO] doped *m*-PBI, the appearance of **c** and **d** proves the existence of $[2\text{-Sema}]^+$, respectively N-methyltaurine in the membrane. Since

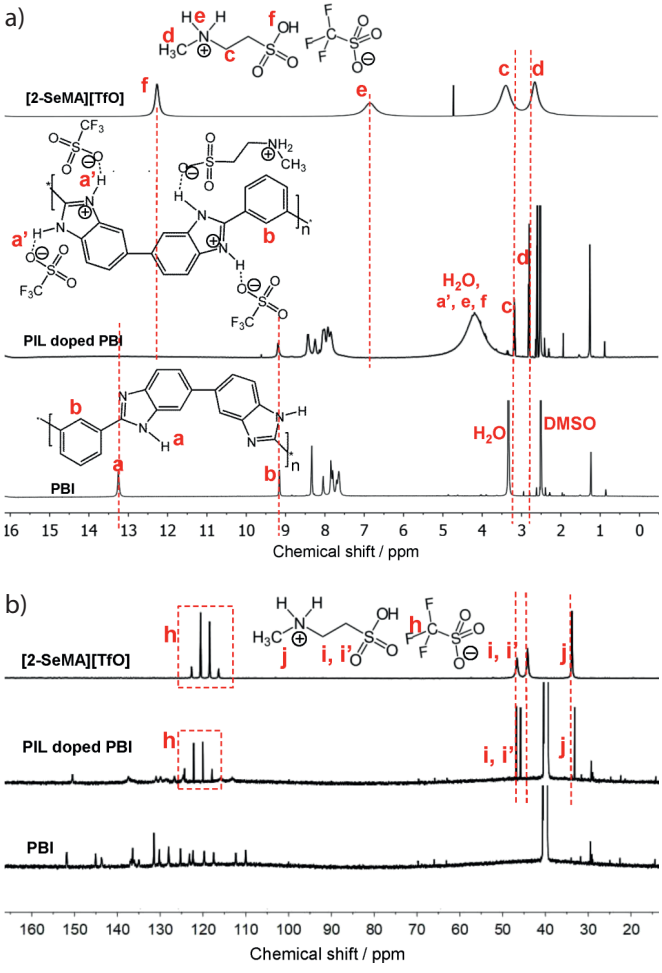

Fig. 7 The (a) ^1H and (b) ^{13}C-NMR spectra of [2-Sema][TfO], PBI and [2-Sema][TfO] doped PBI in DMSO-d6.

$[2\text{-Sema}]^+$ and N-methyltaurine cannot be distinguished by NMR, the observed signals at 2.8 ppm and 3.2 ppm of the methyl protons **d** and ethylene protons **c** could be principally caused by both species. The integration of the signal of the ethylene protons **d** and of the signal of the benzene ring proton **b** (*m*-PBI) yields a doping degree of ~0.36 per *m*-PBI repeat unit regarding $[2\text{-Sema}]^+$, respectively N-methyltaurine (signal area of **c**: **b**≈1.44:1). When assume that the signals **c** and **d** are only caused by N-methyltaurine ($M_{N\text{-methyltaurine}}$=138 g/mol) one would obtain only a mass increase of ~16.1 wt.%. This does not fit to the observations from the TGA measurements where an excess mass increase of 30 wt.% is found in addition to the mass increase of about 100 wt.% due to the formation of polybenzimidazolium triflate *m*-PBI-H_2^+ $(TfO^-)_2$. When assuming that the signals **c** and **d** are caused by [2-Sema][TfO] ($M_{[2\text{-Sema}][TfO]}$=289 g mol^{-1}) one would obtain a mass increase of ~33.8wt.%. This fits much better to the observed value from the TGA measurements. The value calculated by using the NMR data is slightly larger. This may be caused by a small amount of residual N-methyltaurine. The existence of $[TfO]^-$ anions in the membrane can be proved by ^{13}C-NMR, but the spectra cannot be used for quantitative calculations.

There is a slight shift the ethylene and methyl proton signal **c** and **d** when comparing the spectra of the neat PIL and the PIL doped membrane dissolved in DMSO. The high polar PIL [2-Sema][TfO] has no common solvent with *m*-PBI. Thus, the chemical shifts in the spectra of the active protons, such as SO_3H **f**, NH_2^+ **e**, imidazolium **a'** and the H_2O protons, are difficult to compare when using different, respectively no solvent. We assume that due to the high acidity of the $[2\text{-Sema}]^+$ cation a coupling between SO_3H, NH_2^+, imidazolium and H_2O protons occurs, leading to an average signals of all species showing up at 4.2 ppm.

According to the detected fractions of cation, anion and N-methyltaurine, it can be assumed that the free (conjugated) base N-methyltaurine diffuses out after protonation. There are two triflate anions per repeat unit of the PBI chains, which will provide ~95 wt.% weight increase. Thus, a PBI · triflate is formed. The remaining ~30wt.% weight increase is due to the uptake of additional PIL, i.e., [2-Sema][TfO] and some N-methyltaurine. The additional species are absorbed by forming H-bonds in protonated PBI membrane. The low (effective) doping degree regarding the PIL may explained the poor (total) conductivity.

3.7 Analysis of [2-Sema][TfO] Doped PBI Membranes by Light Microscopy

The [2-Sema][TfO] doped PBI membranes were also investigated by light microscopy, a micrograph is depicted in Figure 8. Incremental density of mechanical defects can be observed with increasing doping level, which may cause a decay of the mechanical properties.

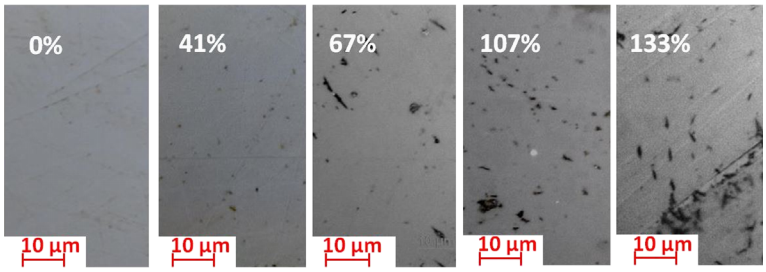

Fig. 8 Images of the [2-Sema][TfO] doped PBI membrane, uptake degree from 0% to 133%.

4 Conclusions

The high-Brønsted acidic proton conducting ionic liquid 2-Sulfoethylmethylammonium triflate [2-Sema][TfO] was investigated in this study. There is evidence that the proton transport mechanism in this PIL with a high acidic cation changes from a vehicular in the case of the neat PIL to a cooperative mechanism as a function of the H_2O concentration.

There is an interaction of the high acidic PIL with *m*-PBI, a polymer with basic moieties, when performing an interdiffusion/swelling experiment. The uptake degree of [2-Sema][TfO] by a PBI membrane – expressed as a weight increase – reaches a value of about 130%. Using a membrane with 60 µm thickness the process takes several days due to a slow interdiffusion. A protonation of the base imidazole moieties takes place but there is an out-diffusion of the neutral base N-methyltaurine after the proton transfer from the cation to the polymer. Proton exchange, respectively an interaction between the polar groups and water can be observed in the NMR spectra, indicating a network of H-bonds in doped PBI. Thus, highly acidic PILs are promising candidates for the use as non-aqueous electrolytes. However, a simple swelling process to immobilize the electrolyte in a host polymer – as used successfully to prepare H_3PO_4/PBI membranes for HT-PEFCs – is no applicable. The resulting (total) conductivity is not sufficient. To reach a higher doping degree solution casting may be an alternative preparation method and should be investigated in a future work.

Acknowledgements

The work is funded by the Helmholtz society. JL is grateful for a grant provided by the China Scholarship Council (Grant No.: 201706060187).

Open access funding enabled and organized by Projekt DEAL.

References

[1] E. Quartarone, P. Mustarelli, *Energy & Environmental Science* **2012**, *5*, 6436.

[2] D. J. Jones, J. Rozière, *Journal of Membrane Science* **2001**, *185*, 41.

[3] Q. Li, J. O. Jensen, R. F. Savinell, N. Bjerrum, *Progress in Polymer Science* **2009**, *34*, 449.
[4] K. Wippermann, J. Wackerl, W. Lehnert, B. Huber, C. Korte, *Journal of The Electrochemical Society* **2015**, *163*, F25.
[5] K. Hsueh, E. Gonzalez, S. Srinivasan, *Electrochimica Acta* **1983**, *28*, 691.
[6] C. Korte, F. Conti, J. Wackerl, P. Dams, A. Majerus, W. Lehnert, *Journal of Applied Electrochemistry* **2015**, *45*, 857.
[7] M. Susan, T. Kaneko, A. Noda, M. Watanabe, *Journal of the American Chemical Society* **2005**, *127*, 4976.
[8] A. Noda, M. Susan, K. Kudo, S. Mitsushima, K. Hayamizu, M. Watanabe, *The Journal of Physical Chemistry B* **2003**, *107*, 4024.
[9] K. Wippermann, J. Giffin, S. Kuhri, W. Lehnert, C. Korte, *Phys Chem Chem Phys* **2017**, *19*, 24706.
[10] K. Wippermann, J. Giffin, C. Korte, *Journal of The Electrochemical Society* **2018**, *165*, H263.
[11] P. Rimmelin, S. Schwartz, J. Sommer, *Organic Magnetic Resonance* **1981**, *16*, 160.
[12] C. Korte, F. Conti, J. Wackerl, P. Dams, A. Majerus, W. Lehnert, *Journal of Applied Electrochemistry* **2015**, *45*, 857.
[13] P. Musto, F. Karasz, W. MacKnight, *Polymer* **1993**, *34*, 2934.
[14] J. A. Asensio, E. M. Sanchez, P. Gomez-Romero, *Chem. Soc. Rev.* **2010**, *39*, 3210.
[15] Q. Li, J. O. Jensen, R. F. Savinell, N. J. Bjerrum, *Progress in Polymer Science* **2009**, *34*, 449.
[16] A. De Angelis, C. Flego, P. Ingallina, L. Montanari, M. Clerici, C. Carati, C. Perego, *Catalysis Today* **2001**, *65*, 363.
[17] D. H. Johnston, D. F. Shriver, *Inorganic Chemistry* **1993**, *32*, 1045.
[18] A. Aslan, S. Ü. Çelik, Ü. Şen, R. Haser, A. Bozkurt, *Electrochimica Acta* **2009**, *54*, 2957.
[19] A. Bozkurt, *Turkish Journal of Chemistry* **2005**, *29*, 117.
[20] S. Liu, L. Zhou, P. Wang, F. Zhang, S. Yu, Z. Shao, B. Yi, *ACS Appl Mater Interfaces* **2014**, *6*, 3195.
[21] R. Bouchet, E. Siebert, *Solid State Ionics* **1999**, *118*, 287.
[22] R. Foglizzo, A. Novak, *Journal de Chimie Physique* **1969**, *66*, 1539.
[23] T. Sarada, R. Granata, R. T. Foley, *Journal of The Electrochemical Society* **1978**, *125*, 1899.
[24] D. R. Lide, *CRC Handbook of Chemistry and Physics*, CRC Press, Boca Raton, FL, USA, **2004**, Vol. 85, pp. 662.

